Simulation of the $^{3}He(n,p)$ Reaction for Nuclear Well Logging Applications

Samanda C. A. Correa, PEN/COPPE/UFRJ & UEZO
Edmilson M. Souza, PEN/COPPE/UFRJ & DEGEO/IGEO/UFRJ
Ademir X. Silva, PEN/COPPE/UFRJ
Inaya C. B. Lima, IPRJ/UERJ
Paula L. F. Rocha, DEGEO/IGEO/UFRJ
Ricardo T. Lopes, PEN/COPPE/UFRJ

This paper was prepared for presentation during the 11th International Congress of the Brazilian Geophysical Society held in Salvador, Brazil, August 24-28, 2009.

Abstract

Computer modeling of neutron well logging instrument responses is becoming a necessity for petro-physical research and oil companies. It serves as a low-cost substitute for experimental test pits, as well as a means for obtaining data that are difficult to obtain experimentally. Neutrons in these tools are generally detected through ^{3}He filled detectors. Detection of neutrons in a ^{3}He counter occurs by means of the (n, p) reaction, yielding a proton and a triton. Computational simulation using the Monte Carlo code MCNP has been considered a powerful tool to simulate the response of neutron porosity tools. In the MCNP code the detection of neutrons in a ^{3}He gas has been making by means of energy functions that convert neutron fluxes to reaction rates (n,p). It allows obtaining count values comparable with experimental data. However, it does not allow producing light ions from neutron capture reactions like triton and proton, and nor study the behavior of these particles as a function of the detector design. With the development of the version MCNPX 2.6, the simulation of light ions (protons, triton) from neutron capture reactions was made possible. The purpose of this work is to use the new capabilities included in the MCNPX 2.6 code to simulate the $^{3}He(n,p)$ reaction for nuclear well logging applications. The results obtained confirm that it is useful to predict the count values, as it allows obtaining results comparable with the literature. Besides, the new capabilities of the MCNPX 2.6 allow producing the triton and proton reaction products and the expected pulse height spectrum from a ^{3}He detector in which the wall effect is significant.

Introduction

The motivation for the development of nuclear well logging techniques in petro-physical research and in oil companies has been mainly the determination of the lithology and fluid characteristics of subsurface rock formations. The radiation interacts with the materials in and around the borehole and sensitive detectors are used to measure the scattered radiation. Interpretations of these measurements are required to assess the properties of the surrounding material. The data interpretations usually are made based on benchmark measurements with the tool in a series of known borehole configurations, information from other logging tools, and detailed radiation transport calculations of the tool in the benchmark and downhole environments.

The purposes of the calculations are to predict and understand the measured results in as much detail as possible. Additional calculations can be used to provide calculated tool responses where measurement standards do not exist. Consequently, environmental corrections to the tool response resulting from changes in downhole conditions can be modeled using accurate radiation transport calculations. These calculations can provide detailed insight into the response of the tool, which is crucial to designing new or improved nuclear tools.

Nuclear well logging problems are difficult radiation transport calculations for several reasons. They are inherently three dimensional and are time dependent for pulsed radiation sources. These problems represent medium-to-deep radiation penetration and often require the coupled neutron/ charged particle/ proton/ photon/ electron transport. Extremely accurate calculational results are needed to extract as much information as possible from measurements. High accuracy requires an accurate representation of the source, a detailed geometric model, the best and most extensive nuclear and atomic data available, and a tally capability to produce appropriate calculated detector responses.

Modeling these problems requires sophisticated multi-dimensional radiation transport techniques like Monte Carlo method.

MCNP is a general purpose Monte Carlo code for calculating the time-dependent continuous-energy transport of neutrons, photons, and electrons in either single particle or coupled particle mode in three-dimensional geometries. The MCNP code with its associated data libraries is equipped to solve these kinds of difficult radiation transport problems.

One of the applications of the MCNP code has been simulating the response of neutron porosity tools. Neutrons in well logging tools are generally detected through ^{3}He-filled proportional counter. Detection of neutrons in a ^{3}He counter occurs by means of the (n,p) reaction, yielding a proton and a triton which share the reaction energy of 765 keV plus the kinetic energy of the incident neutron. The charged particles expend their

energy in the counter gas, producing ionization along the oppositely directed particle tracks.
In the MCNP code the detection of neutrons in a ^{3}He gas has been making by means of energy functions that convert neutron fluxes to reaction rates (n,p) (Briesmeister, 1997). It allows obtaining count values comparable with experimental data. However, it does not allow producing light ions from neutron capture reactions like triton and proton, and nor study the behavior of these particles as a function of the detector design.
With the development of the version MCNPX 2.6 (Pelowitz, 2007), the simulation of light ions (protons, triton, deuterons and alphas) from neutron capture reactions was made possible. With this in mind, the purpose of this work is to use the new capabilities included in the MCNPX 2.6 code to simulate the ^{3}He(n,p) reaction for nuclear well logging applications.

Neutron Detection

In a typical event, a neutron is captured by a ^{3}He atom, which reacts to produce a proton and triton as shown in Figure 1. The kinetic energies of proton (573 keV) and triton (191 keV) sum to the Q-value of 764 keV for the reaction (Knoll, 2000). The range of these energetic daughter particles is a few millimeters at detector gas pressures of a few atmospheres. The energetic daughter particles ionize atoms creating electron-ion pairs as they slow down. The electrons are attracted to the anode with a drift time of a few microseconds across a typical shell diameter. Motion of the charge carriers produces the measured signal pulse that is sensed by the external electrodes.

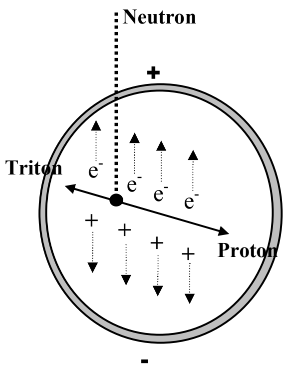

Figure 1: A neutron capture event produces an energetic triton and proton that ionize the stopping gas, producing free electron-ion-pairs.

Charged particles transfer their kinetic energy to the electrons (and a lesser extent the nuclei) along their path. When the proton has higher energies, local charge screening prevents it from transferring as much energy per unit path length as when it is at lower energies, thus spending more time along each interval of its track. The combination of the dependence of the generated electrical pulse on the initial position of the generated free carriers, the relatively large spatial extent of the initial cluster of free electrons, and the tendency of the proton to generate more of its free electrons near the end of its range combines to prevent the development of a distinctive pulse height indicative of neutron interaction. This relatively flat pulse height is what has been observed experimentally.

Computer Model

The calculations were made using the Monte Carlo code MCNPX version 2.6 (Pelowitz, 2007). In order to produce light ions from neutron capture reactions in ^{3}He, the optional neutron capture ion algorithm (NCIA) was used (Hendricks et al., 2007). Besides, the light ion recoil was also considered. It occurs for neutrons and protons colliding with triton and ^{3}He.
Some capabilities that make MCNPX 2.6 useful to well logging applications are listed as follows:

-Complete representation of thermal neutron scattering by molecules and crystalline solids;
-Cross sections for elastic and inelastic scattering;
-Coupled energy/angle distribution for inelastic scattering;
-Angular distributions for elastic scattering;
-Charged ions from neutron capture;
-Neutron models produce light nuclei (A<4).

System Modeling

The results were obtained using a model of a typical nuclear well logging tool, used previously for Serov et al. (1998). It is shown in Figure 2.

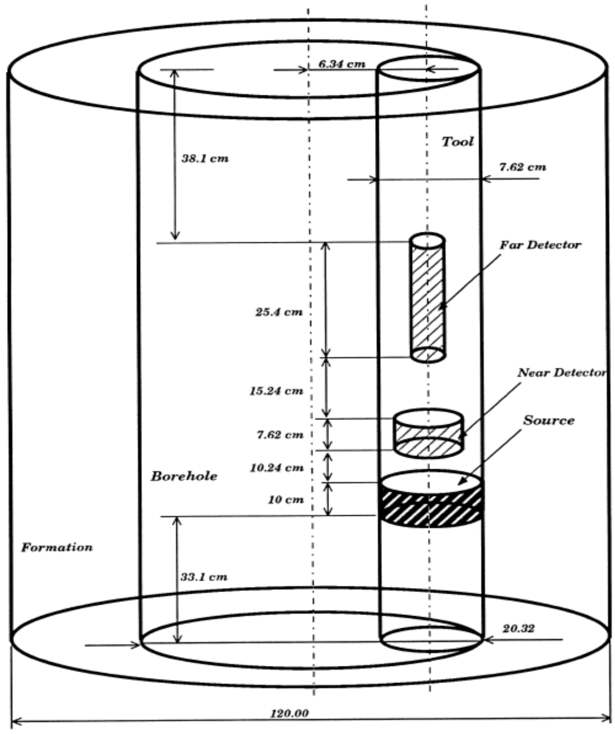

Figure 2: Well logging porosity tool model (not to scale) (Serov et al., 1998).

The formation consists of limestone with 20% porosity. The generic tool is pushed up against the wall of the water borehole. The tool sonde consists of solid iron and contains an Americium-Berylium neutron source. Two detectors with different sizes contain ^{3}He at a pressure of 4 atm, and are placed at different distances from the source along the axis of the tool. The modeled system and the energy spectrum of neutrons used in the simulation can be seen in the Figures 3 and 4.
Two kinds of sources were considered in this work, a point isotropic source in order to obtain the ^{3}He pulse height spectrum, and a point source collimated into a cone of directions in order to obtain the count values.
In the MCNPX calculations the FT8 PHL and F8 tallies were used. The FT option allows the F8 tally to be based on energy deposition in one region via one F6 tally. Thus the F8 tally is dependent on results from another tally, which works because the F8 tally is posted at the end of the particle history where the F6 tally is accumulated along each track of the particle history (Hendricks et al., 2007). The energy output from one region is used to subdivide the pulse height tally (F8). As a result, the anticoincidence is considered.

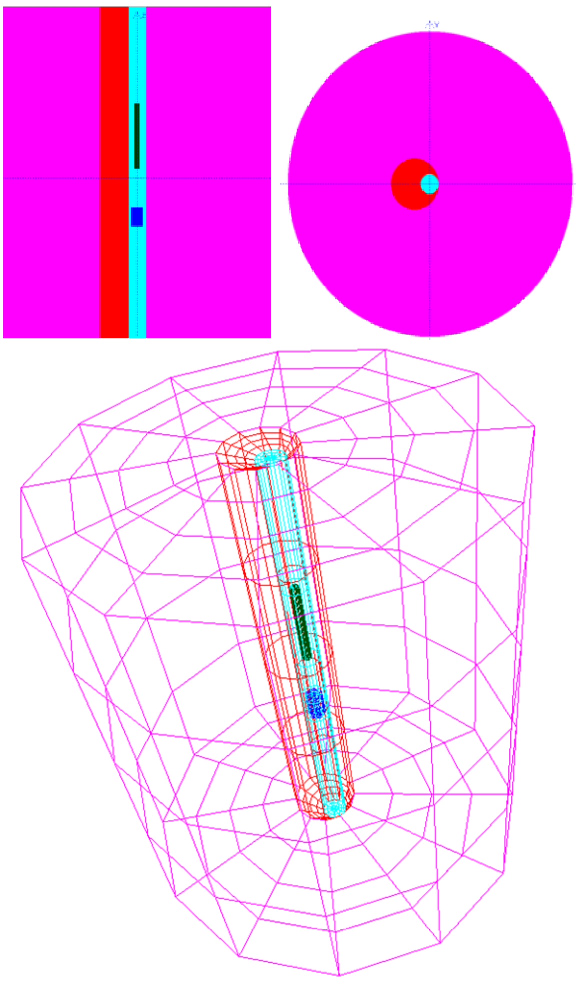

Figure 3: modeled system in the MCNPX 2.6.

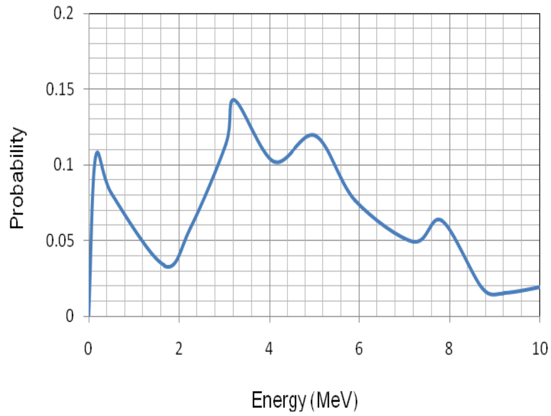

Figure 4: Energy spectrum of neutrons used in the simulation.

Results

Figure 5 shows the ^{3}He pulse height spectrum obtained for the near and far detectors.

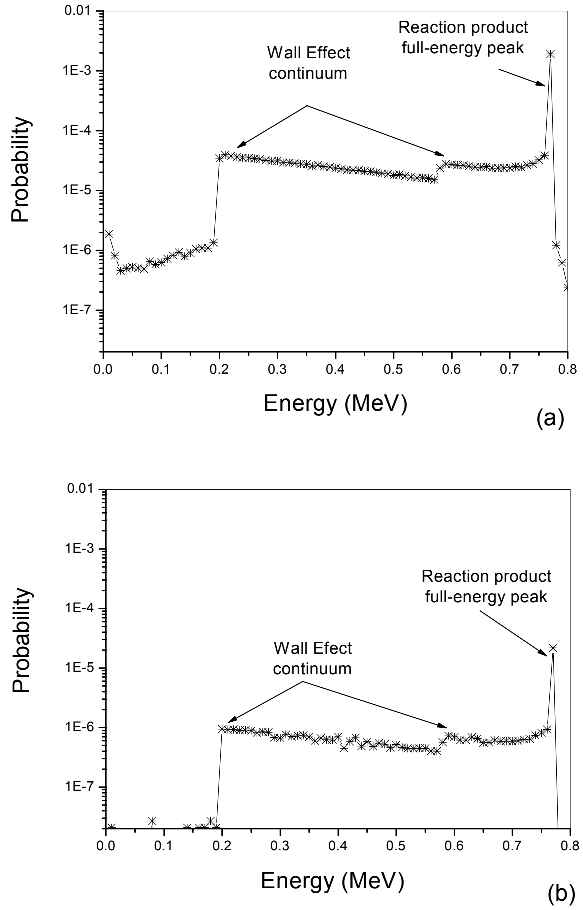

Figure 5: ^{3}He pulse height spectrum. In (a) near detector, and (b) far detection.

For a large tube, nearly all the reactions occur sufficiently far from the walls of the detector to deposit the full energy of the products within the gas. In that event, all energy of the reaction is deposited in the detector. Once the size of the tube is no longer large compared with the range of the proton and triton produced in the reaction, some events no longer deposit the full reaction energy in the gas. If either particle strikes the chamber wall, a smaller pulse is produced. The cumulative effect of this type of process is known as the *wall effect* in gas detector. The two steps or discontinuities in the continuum shown in the Figure 5 is due to this effect.

It can be explained through the following argument. Because the incoming neutron carries no appreciable momentum, the two reaction products must be oppositely directed. If the proton strikes the wall, the triton is therefore directed away from the wall and is very likely to deposit its full energy within the gas. Conversely, if the triton strikes a wall, the entire energy of the proton from that same reaction is usually fully absorbed. Thus, we expect to see wall losses for only one reaction product at a time. There are two possibilities: (1) the proton hits a wall after depositing some fraction of its energy in the fill gas, whereas the triton is fully absorbed in the gas, or (2) the triton hits a wall after depositing part of its energy and the proton is fully absorbed. Under case (1) above, the reaction could occur at a distance from the wall that might be anywhere between zero and full proton range. The amount of energy deposited in the gas can correspondingly vary from (E^{3}_{H} + 0) to (E^{3}_{H} + E_p). Because all locations of the reaction are more or less equally probable, the distribution of deposited energy will be approximately uniform between these two extremes. In the case (2), parallel arguments can be made to show that the energy deposited in the gas will vary from (E_p + 0) to (E_p + E^{3}_{H}). The combined energy deposition distribution of all events in which either reaction product strikes a wall will simply be the sum of the two cases.

In addition to the wall effect events, the sketch above also shows the location of the full energy peak that results from all those reactions from which both products are fully absorbed in the gas. The wall effect continuum extends from E^{3}_{H} (0.191 MeV) up to the full energy peak at E^{3}_{H} + E_p (0.764 MeV).

Besides, Figure 5 also shows that the number of the pulses counted on the near detector is larger. It occurs in particular owing to detection efficiency depends not only on detector properties but also on the details of the counting geometry like the distance from the source to the detector.

In Table 1, the count values obtained in this work using the new capabilities included in the MCNPX 2.6 are compared with the count values obtained by Serov et al. (1998) using the MCNP 4A. The comparison of the results presented in both works shows that the count values obtained in this study are in good agreement with the literature.

Conclusions

The new capabilities included in the MCNPX 2.6 code to simulate the ^{3}He(n,p) reaction for nuclear well logging applications was implemented in this work. The results obtained confirm that it is useful to predict the count values, as it allows obtaining results comparable with the literature. Besides, the new capabilities of the MCNPX 2.6 allow producing the triton and proton reaction products and the expected pulse height spectrum from a ^{3}He detector in which the wall effect is significant. It makes possible studies of the behavior of these reaction products as a function of the ^{3}He detector design.

Acknowledgments

This work was partially supported by *Conselho Nacional de Desenvolvimento Científico e Tecnológico* (CNPQ), *Fundação de Amparo à Pesquisa do Estado do Rio de Janeiro* (FAPERJ) and *Agência Nacional do Petróleo, Gás Natural e Biocombustíveis* (ANP).

References

Briesmeister, J.F., 1997, MCNP: A General Monte Carlo N-Particle Transport Code Version 4B. LA-12625-M, Manual, Los Alamos, USA.

Hendricks, J.S., McKinney, G.W., Fensin, M.L., James, M.R., et al., 2007, MCNPX Version 2.6. LA-UR-07-4137, Los Alamos, USA.

Knoll, G.F., 2000, Radiation Detection and Measurement, Third Edition,John Wiley and Sons, USA.

Pelowitz, D.B., 2007, MCNPX User's Manual Version 2.6. Los Alamos, USA.

Serov, I.V., John, T.M., Hoogenboom, J.E., 1998, A New Effective Monte Carlo Midway Coupling Method in MCNP Applied to a Well Logging Problem. Appl. Rad. Isot., 49, 1737-1744.

Table 1. Comparison of count values for the oil well porosity tool model.

Detector Position		Serov et al.(1998) - MCNP 4A				This work MCNPX 2.6
		Analog continuous	Weight Windows continuous	Analog multigroup	Midway analog multigroup	Analog Continous
Near Detector	Flux x 10^4 per source particle	5.1588	5.0604	4.7046	4.6481	5.2062
Far Detector	Flux x 10^6 per source particle	6.2822	6.3027	4.2633	4.3289	7.3447